# THERMALLY DEVELOPING LAMINAR FLOW AND HEAT TRANSFER CHARACTERISTICS IN A THREE-SIDED CUSPED DUCT

T'Jollyn I.[1,2] *, Nonneman J.[1,2] and De Paepe M.[1,2]
[1]Department of Electromechanical, Systems and Metal Engineering,
Ghent University,
Ghent, 9000,
Belgium.
[2]FlandersMake@UGent – Core lab EEDT-MP,
Leuven, 3000,
Belgium.
E-mail: ilya.tjollyn@ugent.be

## ABSTRACT

This paper reports on simulations of flow and heat transfer in a three-sided cusped duct. Such a duct is formed by the free space between perfectly packed cylinders. Flow and heat transfer in these types of ducts can for example be found in between stacked tubes in heat exchangers, fuel rods in nuclear reactors and in between conductor wires in a coil. Computational fluid dynamics (CFD) simulations for laminar flow were done using Ansys Fluent. Fully developed laminar flow simulations show that the Darcy friction factor times Reynolds number is equal to 26.012 ±0.004 and that the fully developed laminar flow Nusselt number for a constant temperature boundary condition (T) is equal to 0.9163 ±0.0001. For a constant heat flux boundary condition (H2), the Nusselt number is equal to 0.1332 ±0.0001 and thus much lower. This is a result of the pointed ends of the channel where the angle approaches 0° when moving to the end. The wall temperature at the ends of these points is therefore high compared to the bulk temperature and has a significant effect on the average temperature difference and Nusselt number. Simulations of thermally developing flows show that the variation of the Nusselt number in function of the non-dimensional development length is represented well by a correlation similar to the Lévêque approximation for circular ducts.

## INTRODUCTION

For many heat exchangers and other heat transfer applications, compactness is desired because of the high area density and high heat transfer coefficient which give rise to effective heat transfer [1]. Because of the small passages and thus small hydraulic diameters, laminar flows usually occur. Shah and London give an extensive overview of solutions for laminar flow and heat transfer in a multitude of cross section geometries [1]. However, solutions for the heat transfer in a three-sided cusped duct are missing. This duct is formed by the void between the perfect packing of three cylinders with equal diameter. Such ducts can be found between stacked tubes in a heat exchanger, fuel rods in nuclear reactor or between conductors in a winding. Several authors have analysed the flow characteristics of such ducts. Sparrow and Loeffler analysed flow between cylinders with and without spacing, in a triangular or rectangular stacking [2]. Leonard and Lemlich report values of 2.49 for the ratio of maximal velocity to mean velocity and 6.43 for the Fanning friction factor times Reynolds number constant by utilizing a finite difference method [3]. Shih employed a 12-point matching method and stated values of 2.5664 and 6.5033 for the velocity ratio and friction factor-Reynolds number product respectively [4]. This latter constant is significantly lower than that reported for other conventional ducts. Although no values are reported for heat transfer, Shah and London state that the Nusselt number for the three-sided cusped duct will also be significantly lower than that for other conventional ducts [1]. This paper aims to fill the gap in the reporting on the heat transfer characteristics on laminar flow in three-sided cusped ducts by performing computational fluid dynamics simulation (CFD). Both the constant wall temperature and constant wall heat flux boundary conditions are evaluated. Additionally, thermally developing flow is simulated. The resulting Nusselt number values and correlations can be used for future thermal design without requiring numerical simulations.

## NOMENCLATURE

| | | |
|---|---|---|
| $D$ | [m] | Diameter of base circles |
| $D_h$ | [m] | Hydraulic diameter |
| $f$ | [-] | Darcy friction factor |
| $k$ | [W/mK] | Thermal conductivity |
| $L$ | [m] | Duct length |
| $Nu$ | [-] | Nusselt number |
| $P$ | [m] | Perimeter of the duct cross section |
| $p$ | [Pa] | Pressure |
| $Pr$ | [-] | Prandtl number |
| $Q$ | [W] | Heat flow |
| $q$ | [W/m²] | Heat flux |
| $Re$ | [-] | Reynolds number |
| $S$ | [m²] | Duct cross-sectional area |
| $T$ | [K] | Temperature |
| $V$ | [m³/s] | Volumetric flow rate |
| $v$ | [m/s] | Velocity |
| $x$ | [m] | Flow length |
| $x^*$ | [-] | Non-dimensional development length |

Special characters

| | | |
|---|---|---|
| $\theta$ | [-] | Non-dimensional temperature |
| $\nu$ | [m²/s] | Kinematic viscosity |
| $\rho$ | [kg/m³] | Density |

Subscripts

| | |
|---|---|
| $b$ | Bulk |
| $H2$ | Constant heat flux boundary condition |
| $max$ | Maximal |
| $m$ | Mean |
| $T$ | Constant temperature boundary condition |
| $w$ | Wall |
| $x$ | Local |

## SIMULATION METHODOLOGY

### Geometry

The geometry considered in this paper is a three-sided cusped duct, as shown in Figure 1. This is the void formed by perfect packing of three cylinders with equal diameter. The geometry has three sides and three end points, where the angle between the sides approaches zero when moving towards the end. As this geometry has three symmetry planes, only one sixth is numerically simulated to reduce the required computational time, as shown in Figure 2.

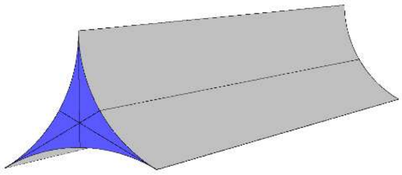

**Figure 1** Three-sided cusped duct geometry

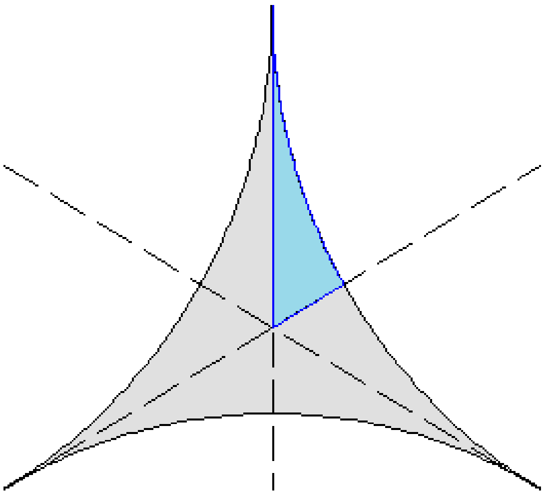

**Figure 2** Cross-sectional view of the three-sided cusped duct with symmetry planes (dashed lines) and simulation domain (blue)

The cross-sectional perimeter $P$ and area $S$ are determined using the circle diameter $D$ (equal to 0.1 m in the following simulations) by equations (1) and (2) respectively. From these parameters, the hydraulic diameter $D_h$ of the duct can be derived as a function of the circle diameter as in equation (3).

$$P = \pi/2\ D \tag{1}$$

$$S = (2\sqrt{3} - \pi)/8\, D^2 \tag{2}$$

$$D_h = 4S/P\ = (2\sqrt{3}/\pi - 1)\, D = 0.103\, D \tag{3}$$

### Boundary conditions

For the fully developed flow simulations, a periodic boundary condition is used for inlet and outlet, where the outlet velocities and scaled temperatures are wrapped to the inlet. The temperatures are scaled such that the bulk temperature at the inlet is equal to 300 K. For the heat transfer problem, two different boundary conditions are used: constant wall temperature (T boundary condition) of 310 K and constant wall heat flux (H2 boundary condition) of 10 kW/m². A pressure drop of 10 kPa/m is imposed over the length of the duct.

To evaluate the heat transfer for thermally developing flow, a uniform fluid temperature of 300 K is applied at the inlet. As the goal is to only investigate the thermal development effect, the velocity profile applied at the inlet is the profile determined in the fully developed flow simulations. The outlet has a uniform pressure.

### Numerical method

The commercial software Ansys Fluent is used for the CFD simulations of the flow and heat transfer in the three-sided cusped duct. Laminar and steady-state simulations are performed, as this is the flow regime of interest. The governing equations to be solved are the continuity, momentum and energy equations. The Reynolds number used is the simulations is equal to 83, which is sufficiently low. The mass, momentum and energy conservation equations are solved using second order discretization schemes.

To discretize the fluid domain, first a surface mesh of quadrilateral elements with a size of 0.05 mm is made of the inlet. This mesh is swept along the length of the duct to create hexahedral elements. For the fully developed flow simulations, this results in a mesh with 127400 cells. For the developing simulations, the surface mesh is swept along a length of 0.4 m with a spacing of 1 mm, resulting in a domain consisting of 10.5 million cells. Calculations were done on a single core of an Intel Xeon E5-2690v4 with 2.6GHz CPU and 128GB 2400MHz ECC memory. For the fully developed flow cases, simulation time for a single case was about 8 minutes. The simulation's duration was around 8 hours for the developing flow case.

The grid convergence is verified using the grid convergence index (GCI) as defined by Roache [5]. The grid discretization error is determined for the fully developed flow simulation with a constant temperature boundary condition. A coarse mesh with an element size of 0.1 mm and 33095 cells is used to calculate the Darcy friction factor and Nusselt number. The results for both the coarse and fine mesh are shown in Table I. The GCI for the fine grid as defined by Roache is equal to 0.03% for the friction factor and 0.01% for the Nusselt number.

**Table I** Grid convergence index

| | Coarse | Fine | GCI (%) |
|---|---|---|---|
| $f$ | 0.31261 | 0.31271 | 0.03 |
| $Nu$ | 0.91635 | 0.91629 | 0.01 |

## FULLY DEVELOPED FLOW

### Flow and friction factor

The simulation results are first validated for the flow characteristics and friction factor with the values reported by Shih [4]. The velocity field in a cross section of the duct is shown in Figure 3. As expected, the velocities in the pointed ends are close to zero, due to the very narrow flow passage there. The maximal velocity $v_{max}$ is related to the average velocity $v_m$ by equation (4), where the average velocity is defined as the volumetric flow rate divided by the duct cross-sectional area. The ratio of 2.5662 ±0.0008 corresponds well with the value of 2.5664 reported by Shih [4].

$$v_{max} = 2.5662\ v_m \tag{4}$$

For fully developed laminar flow in a straight duct, the product of the Darcy friction factor $f$ and Reynolds number $Re$ is a constant. This constant can be determined using equations (5) and (6), where the volumetric flow rate $V$ is gathered from the numerical simulations.

$$f = \frac{\Delta p}{L} \frac{2\, S^2}{\rho\, V^2} D_h \tag{5}$$

$$Re = \frac{V\, D_h}{S\, \nu} \tag{6}$$

In equations (5) and (6), $\Delta p$ is the pressure drop, $L$ is the duct length, $\rho$ is the fluid density and $\nu$ is the fluid kinematic viscosity. The constant calculated from the simulations is equal to 26.012 ±0.004, which corresponds with 26.013 (four times the Fanning friction factor) reported by Shih [4]. Overall, the simulations of the flow field closely match the results reported in literature.

**T boundary condition**

The temperature profile is represented by the non-dimensional temperature $\theta$, which is defined by equation (7), where $T$ is the local fluid temperature, $T_b$ is the fluid bulk temperature and $T_w$ is the wall temperature.

$$\theta = \frac{T - T_b}{T_w - T_b} \tag{7}$$

Figure 4 shows the temperature profile for fully developed flow with the constant temperature boundary condition. Due to the low velocities at the end points, the temperature is very close to the wall temperature at these points. In the centre of the duct, a low temperature core with higher velocities is formed.

By integrating the total heat flow at the wall $Q$ from the simulation results, the Nusselt number $Nu_T$ is determined by equation (8), wherein $k$ is the fluid thermal conductivity.

$$Nu_T = \frac{Q}{P\, L\, (T_w - T_b)} \frac{D_h}{k} \tag{8}$$

The Nusselt number is determined here as 0.9163 ±0.0001, which is significantly lower than the fully developed laminar flow Nusselt numbers for ducts with other shapes. This is related to the pointed ends which increase the heat transfer area, but which due to the low fluid velocity in that region do not contribute significantly to the heat transfer. This low Nusselt number was also predicted by Shah and London [1], although no value was determined at that time.

**H2 boundary condition**

For the constant heat flux boundary, the fully developed flow non-dimensional temperature profile is shown in Figure 5. The non-dimensional temperature is determined using equation (7), where the wall temperature is area-averaged as it is no longer constant. Due to the low flow velocities in the end points, the temperature of the wall is very high, as the heat transfer in the slow-moving fluid is very poor.

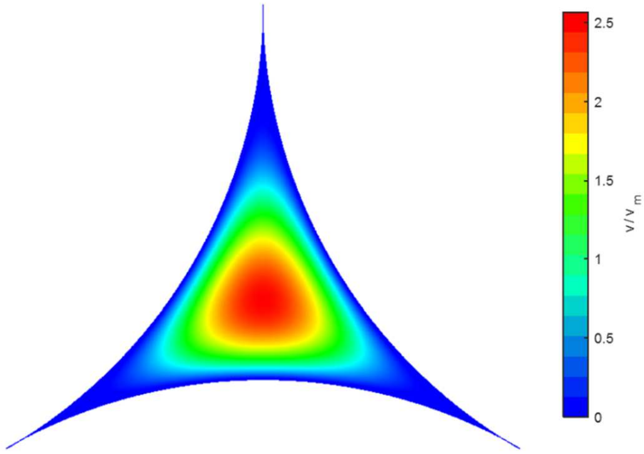


**Figure 3** Fully developed flow velocity profile

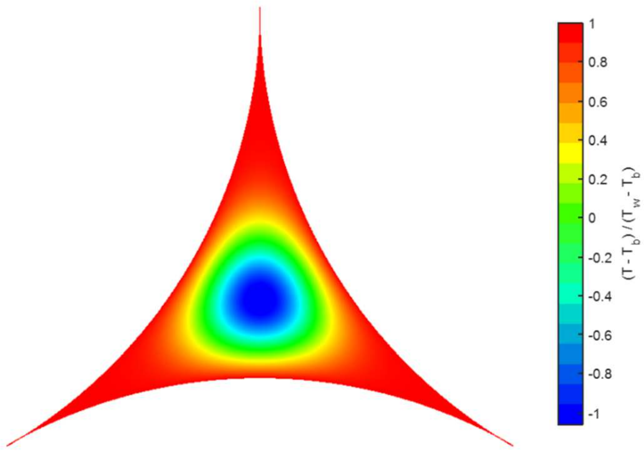


**Figure 4** Non-dimensional temperature profile for fully developed flow with T boundary condition

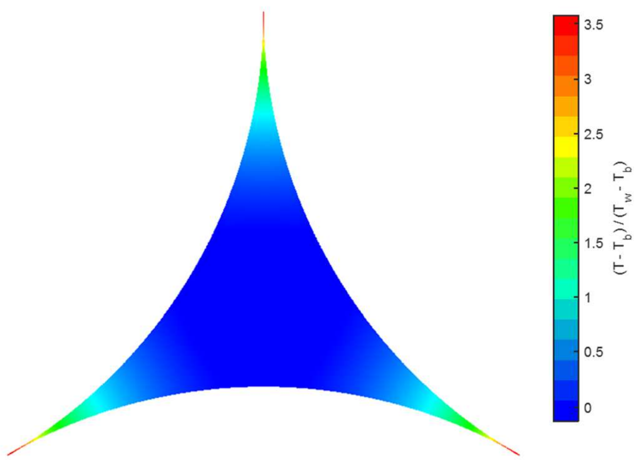


**Figure 5** Non-dimensional temperature profile for fully developed flow with H2 boundary condition

By calculating the area-averaged wall temperature $T_w$ from the simulation results, the Nusselt number $Nu_{H2}$ can be determined using equation (9), wherein $q$ is the wall heat flux.

$$Nu_{H2} = \frac{q}{(T_w - T_b)} \frac{D_h}{k} \tag{9}$$

The Nusselt number for the constant heat flux boundary condition is equal to 0.1332 ±0.0001, which is extremely low due to the poor heat transfer from the end points to the centre of the duct. It is significantly lower than that for the constant temperature boundary condition, as in this case, a heat flux is imposed also on the pointed ends of the geometry. As the flow is almost stationary there, heat transfer will only occur through conduction of the very thin fluid layer. This results in a large thermal resistance from the tips of the geometry to the bulk flow area, resulting in a locally high wall temperature. As the pointed ends make up a significant part of the total perimeter, this leads to an increase in the area-averaged wall temperature and thus a decrease in the Nusselt number.

**Validation and results overview**

Table II gives an overview of the flow and heat transfer characteristics determined in this work and those reported by Shih [4].

**Table II** Three-sided cusped duct flow and heat transfer characteristics

| | $v_{max}/v_m$ | $f\,Re$ | $Nu_T$ | $Nu_{H2}$ |
|---|---|---|---|---|
| Shih [4] | 2.5664 | 26.013 | / | / |
| This work | 2.5662 | 26.012 | 0.9163 | 0.1332 |

## THERMALLY DEVELOPING FLOW HEAT TRANSFER

For laminar flows, the developing flow effect at the inlet of the duct can have a significant effect on the overall heat transfer coefficient in the duct. In these simulations, only the thermal development effect is taken into account. At the inlet of the duct, a fully developed velocity profile is applied, based on the simulations with a periodic boundary condition. The fluid at the inlet has a uniform temperature of 300 K. The T boundary condition is applied by imposing a constant wall temperature of 310 K. The fluid Prandtl number used in the simulation is equal to 1. This value is chosen as it is in between those of commonly used fluids air and water. Furthermore, using the non-dimensional development length (see equation (11)), the results can be easily used for fluids with other Prandtl numbers.

Figure 6 shows the development of the temperature profile along the length of the duct. At the inlet, a uniform fluid temperature is applied. Further on, a boundary layer starts to develop near the wall, which grows thicker when moving away from the inlet. At the outlet, the bulk temperature of the fluid has increased significantly and the temperature profile in the cross section approaches the fully developed flow temperature profile.

The local Nusselt number $Nu_x$ is determined from the simulation results by using equation (10). This equation uses the integrated wall heat flow $Q(x)$ at different location along the flow length $x$. Furthermore, the bulk temperature along the flow length $T_b(x)$ is determined by calculating the mass-averaged temperature of the cross section of the duct along the flow length. $\Delta x$ is the discretization length along the flow direction, which is equal to 1 mm.

$$Nu_x = \frac{Q(x)}{P\,\Delta x\,[T_w - T_b(x)]} \frac{D_h}{k} \tag{10}$$

Figure 7 plots the local Nusselt number as a function of the non-dimensional development length $x^*$, which is defined by equation (11), where $Pr$ is the fluid Prandtl number.

$$x^* = \frac{x}{D_h\,Re\,Pr} \tag{11}$$

From Figure 7, the fully thermally developed flow length can be estimated as $x^* = 0.3$, which is higher than those reported for circular tubes ($x^* = 0.0335$) [6]. This is consistent with other

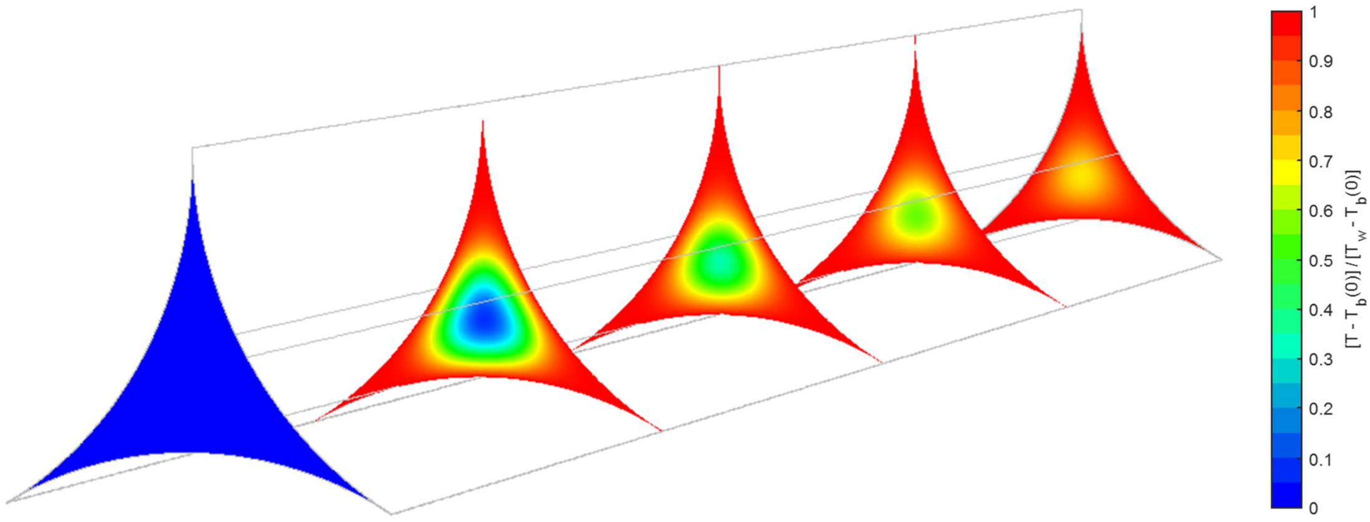


**Figure 6** Non-dimensional temperature profile at different flow lengths ($x$ = 0m; 0.1m; 0.2m; 0.3m; 0.4m)

geometries with lower Nusselt numbers than that of a circular tube, which also have longer fully thermally developed flow lengths. For three-sided cusped ducts at $x^* > 0.3$, the flow can be approximated to be fully developed and the local Nusselt number can be estimated as the fully developed flow Nusselt number. At low $x^*$ (< 0.05), the local Nusselt numbers can be approximated by equation (12).

$$Nu_x = 0.48\, {x^*}^{-\frac{1}{3}} \tag{12}$$

The same value for the exponent in this equation is found as for the well-known Lévêque approximation for thermally developing laminar flow in a circular tube [1]. The correlation for the mean Nusselt number of equation (13) for $x^* < 0.05$ is then determined from equation (12).

$$Nu_m = 0.72\, {x^*}^{-\frac{1}{3}} \tag{13}$$

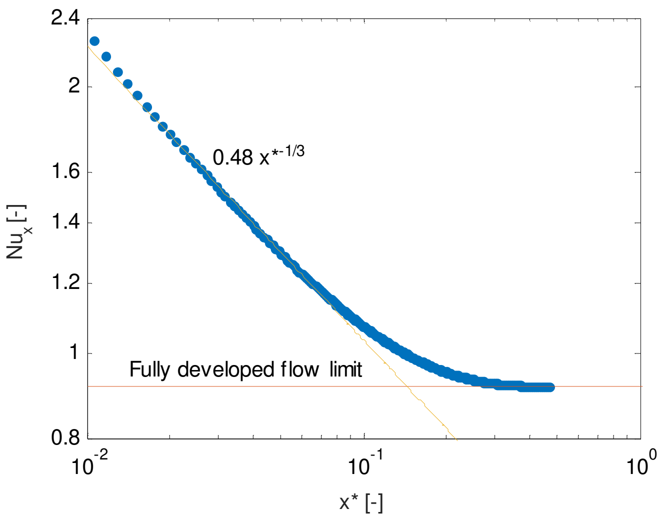


**Figure 7** Local Nusselt number for thermally developing flow with T boundary condition

## CONCLUSION

This paper reports on computational fluid dynamics simulations of laminar flow and heat transfer in three-sided cusped ducts. The validity of the simulations is confirmed by comparing the results of the flow simulations to those reported in scientific literature. The fully developed laminar flow Nusselt number for the constant temperature boundary condition is calculated as 0.9163 ±0.0001, while that of the constant heat flux boundary conditions is determined as 0.1332 ±0.0001. Both these values are considerably lower than those of fully developed flow in other cross section geometries, due to the pointed ends where the angle goes down to 0°. These zones have a significant heat transfer area, but due to the very low velocities heat transfer from and through these zones is poor. Next to fully developed flow, thermally developing flow was numerically simulated. A correlation for the local Nusselt number is proposed as a function of the non-dimensional development length, similar to the Lévêque approximation for thermally developing flow in a circular tube. The reported Nusselt number values and correlations can be used in future thermal designs which include these type of ducts, without the need for time-consuming numerical simulations.

## REFERENCES


[1] Shah R.K. and London A.L., Laminar flow forced convection in ducts: a source book for compact heat exchanger analytical data, Academic Press, 1978

[2] Sparrow E.M. and Loeffler Jr A.L., Longitudinal laminar flow between cylinders arranged in regular array, *American Institute of Chemical Engineers Journal*, Vol. 5, No. 3, 1959, pp. 325-330

[3] Leonard R.A. and Lemlich R., Laminar longitudinal flow between close-packed cylinders, *Chemical Engineering Science*, Vol. 20, No. 8, 1965, pp. 790-791

[4] Shih F.S., Laminar flow in axisymmetric conduits by a rational approach, *The Canadian Journal of Chemical Engineering*, Vol. 45, No. 5, 1967, pp. 285-294

[5] Roache P.J., Quantification of uncertainty in computational fluid dynamics, *Annual review of fluid Mechanics*, Vol. 29, No. 1, 1997, pp. 123-160

[6] Shah R.K. and Sekulic D.P., Fundamentals of heat exchanger design, John Wiley & Sons, 2003